ELSEVIER

Journal of Photochemistry and Photobiology A: Chemistry 148 (2002) 365–374

Journal of Photochemistry and Photobiology A:Chemistry

www.elsevier.com/locate/jphotochem

Water treatment using nano-crystalline TiO_2 electrodes

J.A. Byrne*, A. Davidson, P.S.M. Dunlop, B.R. Eggins

Photocatalysis Research Group, Faculty of Science, University of Ulster at Jordanstown, Room 1F09, Newtownabbey, Co. Antrim, BT37 0QB UK

Received 24 July 2001; received in revised form 4 September 2001; accepted 4 September 2001

Abstract

The photocatalytic and electrochemically assisted photocatalytic degradation of formic acid was investigated in an one-compartment photoelectrochemical cell incorporating nano-crystalline TiO_2 electrodes prepared by the immobilisation of Degussa P25 on tin oxide coated glass. The application of +1.0 V (SCE) to the TiO_2 electrode resulted in a marked increase in the rate of formic acid degradation under anaerobic and air sparged conditions as compared to the open circuit electrode. When the solution was sparged with O_2 the application of a positive bias did not result in a major increase in the rate. A second cathode compartment was added to the cell for the simultaneous photocatalytic oxidation of formic acid and the recovery of copper ions from solution. Formic acid was degraded at the TiO_2 photoanode and copper metal was recovered at the copper mesh cathode with a high efficiency. © 2002 Elsevier Science B.V. All rights reserved.

Keywords: Titanium dioxide; Photocatalysis; Water treatment; Formic acid

1. Introduction

The use of photocatalysis as an alternative or complementary technology for the treatment of polluted water has been widely reported [1]. The use of TiO_2 in suspension or slurry type reactor requires a post-treatment catalyst recovery stage. Alternatively the catalyst may be immobilised onto a suitable solid support matrix which eliminates the need for post-treatment removal [2]. If the supporting substrate is electrically conducting the result is a photoanode and this may be incorporated into an one- or two-compartment photoelectrochemical cell (PEC) in which the oxidation and reduction sites are physically separated. In an one-compartment cell the anode and cathode electrodes are separated only by solution and the application of an external electrical bias may be used to electrochemically assist the photocatalytic oxidation of organic pollutants in water. Indeed other workers have investigated electrochemically assisted photocatalysis (EAP) and have reported significant increases in the degradation efficiency of aqueous organic substances with the application of a small positive electrical bias to the working TiO_2 electrode with O_2 acting as the electron acceptor [3–16]. In addition the electrochemical measurements in such a system provide valuable information into the mechanism of the photocatalytic process.

In one-compartment PECs the electron acceptor is normally dissolved O_2. In theory, any species with a reduction potential more positive than the flat band potential of the TiO_2 ($E_{fb} \sim -0.7$ V (SCE) at pH 7) can be reduced. Indeed, the use of TiO_2 suspension reactors has been reported for the recovery of metals [17,18], however, this system suffers from many disadvantages i.e. metal recovery necessary, short-circuiting by oxidation of previously reduced metal species, and screening of light from the catalyst by the deposited metal. If one incorporates the TiO_2 anode into a two-compartment PEC the oxidation and reduction sites are physically separated either by a membrane, salt-bridge, or porous frit, which prevents mixing of the solutions but which allows the flow of electrical charge. In this system photogenerated electrons may move from the photoanode via an external circuit to the cathode where a desired reduction reaction can take place e.g. the reduction of metal ions. The feasibility of using a two-compartment PEC for the simultaneous oxidation of organic pollutants in one-compartment and the recovery of dissolved metal ions in a second compartment has been demonstrated previously [19]. Mbindyo et al. [20] reported pollutant decomposition with simultaneous generation of hydrogen at the cathode in a two-compartment PEC.

The objective of this work is to take one step further toward the actual application of photoelectrochemical technology for the treatment of polluted water. The design of any electrolysis cell must take into account that the process requires the energy intensive use of electricity. Therefore, one must ensure that every aspect must be explored in order to

* Corresponding author. Tel.: +44-28-9036-6224; fax: +44-28-9036-6028.
E-mail address: j.byrne@ulst.ac.uk (J.A. Byrne).

1010-6030/02/$ – see front matter © 2002 Elsevier Science B.V. All rights reserved.
PII: S1010-6030(02)00064-3

increase the energy efficiency of the process. The cell voltage is a complex quantity made up of a number of terms.

$$E_{\mathrm{CELL}} = E_{\mathrm{e}}^{\mathrm{C}} - E_{\mathrm{e}}^{\mathrm{A}} - |\eta_{\mathrm{A}}| - |\eta_{\mathrm{C}}| - IR_{\mathrm{CELL}} - IR_{\mathrm{CIRCUIT}} \quad (1)$$

where $E_{\mathrm{e}}^{\mathrm{C}}$ and $E_{\mathrm{e}}^{\mathrm{A}}$ are the equilibrium potentials for the anode and cathode reactions, respectively. In electrolytic processes the overpotentials and *IR* terms represent energy inefficiencies and hence will make the cell voltage a larger negative value. $E_{\mathrm{e}}^{\mathrm{C}} - E_{\mathrm{e}}^{\mathrm{A}}$ is the fraction of the cell voltage which, cannot be avoided. η_{A} and η_{C} are the anode and cathode overpotentials, respectively. In the case of a photocatalytic anode the overpotential required for the oxidation of the organic pollutant is met by the energy of the absorbed photons i.e. the reduction potential of a valence band hole in TiO_2 is +2.5 V (SCE) at pH 7. In an one-compartment cell for electrochemically assisted photocatalytic oxidation of organic pollutants the electron acceptor is normally dissolved O_2. Platinum is the material of choice for O_2 reduction but it is too expensive for use in large-scale applications. Platinised titanium mesh, which is much cheaper, is used widely in industrial electrochemical cells and therefore may be a suitable material for use as a counter electrode (CE) for EAP. For a PEC the IR_{CELL} may be minimised by orientating the electrodes as close as possible with the TiO_2 anode facing the cathode. This may be accomplished by the use of a TiO_2–tin oxide glass plate electrode under back-face illumination facing a Pt–Ti mesh CE of similar geometry.

In this work an one-compartment PEC was designed and constructed which incorporated a nano-crystalline TiO_2–tin oxide glass electrode and a Pt–Ti mesh CE in a flat plate configuration. The reactor was used to investigate rate of degradation of formic acid with the TiO_2 electrode at open circuit (OC) and for EAP. The cell was also adapted by the inclusion of a second (cathode) compartment separated from the anode using an anion exchange membrane. This two-compartment cell was used for the simultaneous photocatalytic oxidation of formic acid at the anode and the recovery of dissolved copper ions as copper metal at a copper mesh CE.

2. Experimental

2.1. Preparation of TiO_2 electrodes

TiO_2 electrodes were prepared by the electrophoretic deposition of Degussa P25 on indium doped tin oxide (ITO) soda lime glass (Donnelly, USA) and fluorine doped tin oxide (FTO) soda lime glass (Pilkington K glass) followed by heat treatment at 673 K to effect particle adhesion and cohesion. Details of the electrophoretic coating procedure have been reported previously [2]. An electrical contact was made to the surface of the ITO not coated with TiO_2 using silver loaded conducting epoxy and a copper wire. The catalyst loading was $1.0 \pm 0.2\ \mathrm{mg\ cm^{-2}}$.

2.2. One-compartment flow reactor

The sandwich type reactor was made from perspex which was machined to give the required dimensions. A schematic representation of the reactor is shown in Fig. 1. The CE was made from platinised titanium mesh (Pt–Ti mesh, PC Tita-

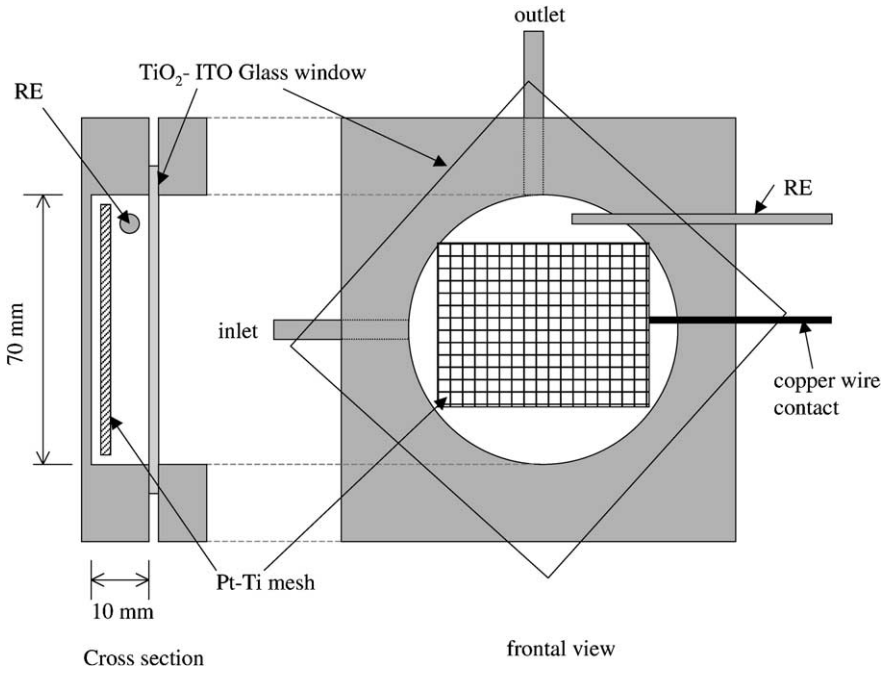

Fig. 1. A schematic representation of the one-compartment flow cell.

nium, UK) and the reference electrode (RE) was a miniature saturated calomel electrode (SCE). Stainless steel inlet and outlet ports were set in the reactor at right angles to each other. The inlet and outlet ports were attached to a water-jacketed glass reservoir incorporating a sample port and a glass frit for gas purging. The water in the reactor was re-circulated through the reactor using a variable speed peristaltic pump (Watson Marlow, MHRE 200). The cell volume was 35 cm^3 with the Pt–Ti mesh CE in place. The total operating volume of the reactor was 72 cm^3. The temperature of the reactor solution was thermostated to 293 K during the experiments. Two Philips TLD 18 W/08 UVA lamps (peak emission $\lambda = 370$ nm) were positioned 40 mm from the glass window. The illuminated area of the TiO_2 electrode was 38 cm^2 and the incident light intensity was determined by ferrioxalate actinometry to be 2.14×10^{-8} einstein s^{-1} cm^{-2}.

Formic acid was used as the model pollutant and was added to the reactor at an initial concentration of 3.18×10^{-3} mol dm^{-3} (pH 3.2) or 6.36×10^{-3} mol dm^{-3} (pH 3.0). In a typical experiment 72 cm^3 of formic acid solution was added to the reactor and re-circulated through the reactor at a flow rate of 60 cm^3 min^{-1} in the dark for 15 min. At the same time the lamps were switched on and allowed to warm up. The reservoir was purged with O_2, air, or oxygen free nitrogen (OFN) during both the dark equilibration period and for the duration of the experiment. Samples were removed form the reservoir at $t = 0$ min and thereafter every 15 min for analysis. The concentration of formic acid in the samples was determined by HPLC using an Aminex HPX-87H ion exclusion column (300 × 7.8 i.d., Biorad) with guard column, a P2000 pump, AS1000 autosampler, LIS UV/Vis detector, and PC1000 software (Thermoquest). The HPLC conditions were as follows: mobile phase was 10^{-1} mol dm^{-3} H_2SO_4 at a flow rate of 0.8 cm^3 min^{-1}; 100 μl injection loop; detection at $\lambda = 210$ nm.

The electrode potential and short-circuit current were recorded using a multimeter with data logging function (Keithly). A potentiostat with PC control (Sycopel AEW2) was used for linear sweep voltammetry (LSV), OC potential measurements, and for potentiostatic control of the cell and current measurements in fixed potential experiments.

2.3. Two-compartment flow reactor

A second compartment was added to the one-compartment reactor as shown in Fig. 2. The working electrode was a TiO_2–FTO glass electrode which was short-circuited to the CE electrode in the cathode compartment which was made from four pieces of fine copper mesh with a copper wire contact. The volume of the anode was 38 cm^3 and the volume of the cathode with the copper mesh CE in place was 26 cm^3. Separate reservoirs were used for the anode and cathode compartments. The total reactor volumes of anode and cathode half cells were 72 and 64 cm^3, respectively. The anode and cathode compartments were separated by an anion exchange membrane (BDH). The liquid in both

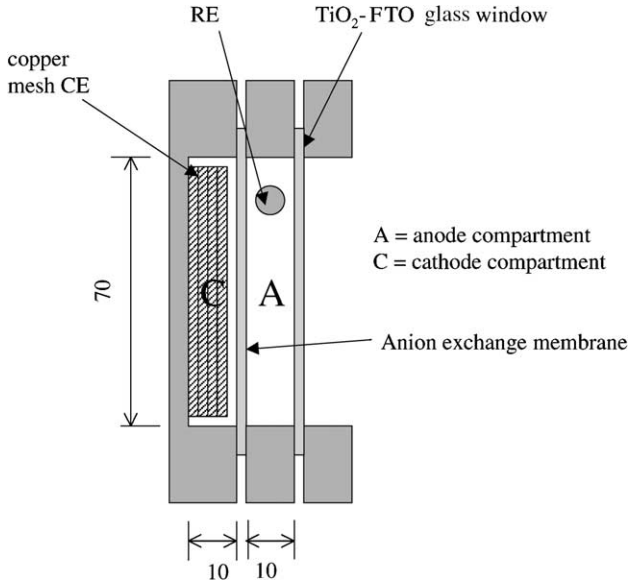

Fig. 2. A schematic representation of the two-compartment flow cell.

compartments was re-circulated through the reservoirs at the same flow rate (60 cm^3 min^{-1}) using a dual head peristaltic pump (Cole Palmer 7553-75). The potential of the anode was measured against an SCE inserted in the anode compartment and the short-circuit current was recorded using a data logging multimeter as above. Both reservoirs were purged with OFN prior to and during experiments. The temperature of the reactor solutions was thermostated to 293 K during the experiments. The UVA source was two Philips TLD 18 W/08 lamps positioned 40 mm from the glass window.

An amount of 72 cm^3 of formic acid (6×10^{-3} mol dm^{-3}, pH 3.0) was added to the anodic half cell and 64 cm^3 of copper (II) nitrate (6×10^{-3} mol dm^{-3}) was added to the cathodic half cell (pH was adjusted to 3.0 using HNO_3). KNO_3 was present as the supporting electrolyte in both compartments at 0.5 mol dm^{-3}. The solutions were re-circulated for 15 min while the reservoirs were purged with OFN and the lamps were allowed to warm up. A sample was then removed from the anode reservoir at $t = 0$ and the anode was illuminated. Samples were withdrawn every 30 min thereafter for a period of 120 min. The concentration of formic acid was determined using the HPLC method as above. The amount of copper recovered was determined by gravimetric analysis of the copper mesh CE at the end of the experiment.

3. Results and discussion

3.1. Photocatalytic oxidation of formic acid

Formic acid was used as the model pollutant in this study because: (1) it is oxidised directly to CO_2 without the formation of any stable intermediate products; (2) it is an intermediate in the photocatalytic degradation of other larger organic

compounds; (3) it has been used previously in photocatalytic and EAP studies [10,11,16]. Formic acid has previously been reported to act as a current doubling agent [21,22] on semiconductor electrodes, with an one electron oxidation yielding a $CO_2^{\bullet -}$ radical which can then inject a second electron into the conduction band of the semiconductor. Previously we reported that the formate ion was an efficient hole scavenger at the surface of illuminated nano-crystalline TiO_2 electrodes where its presence resulted in large increases in the anodic photocurrent over that for electrolyte alone [23]. Formic acid is electrochemically oxidised by a $2e^-$ oxidation to yield CO_2 at a potential of +0.3 V on a smooth Pt electrode [24].

3.2. Photoelectrochemical response of the electrode

The current–potential (*I–E*) response of the electrode was measured using LSV in the presence of formic acid before each fixed potential experiment (Fig. 3). For these electrodes the dark current was negligible below +1.0 V, but upon illumination there was an increase in the anodic current. The photocurrent increased linearly with increasing positive potential up to +2.0 V. The *I–E* response under illumination for the air and OFN sparged solutions is practically the same (Fig. 3 (1) and (2)), however, the photocurrent response in O_2 saturated conditions is lower (Fig. 3 (3)) and this is due to two main reasons: (1) O_2 scavenges conduction band electrons from the nano-crystalline film before they reach the contact electrode [25]; (2) O_2 reacts with the primary radical formed by the one electron oxidation of formic acid [23]. In the air sparged solution the photocurrent quenching effect may have been balanced by a more favourable cathodic reduction of O_2 as compared to the OFN sparged solution, thus resulting in high photocurrent. In O_2 sparged solutions the photo-quenching was much greater.

3.3. Photocatalytic and electrochemically assisted photocatalytic oxidation of formic acid

We have reported previously that the electrophoretic immobilisation of Degussa P25 onto a conducting support results in electrodes which behave as microporous nano-crystalline TiO_2 electrodes [23,25]. Charge separation in nano-sized photo-active particulate films is achieved from the differing rates of electron and hole transfer at the solution interface [3]. Micro-porous nano-crystalline TiO_2 electrodes lend themselves to environmental applications because of the large surface area of catalyst available for reaction. Electron transport in nano-crystalline TiO_2 electrodes occurs via diffusion and is not potential dependent, however, the fermi energy level of the contact electrode is potential dependent. The application of a positive potential serves to lower the fermi energy level of the contact electrode, increasing the efficiency of electron removal from the illuminated particulate film, therefore increasing quantum efficiencies.

The main objective was to determine if the application of an external electrical bias to the photoanode resulted in an increase in the degradation rate of formic acid in an one-compartment cell. Gerischer and Heller [26] previously reported that where O_2 is acting as the electron acceptor the removal of conduction band electrons may be slow therefore resulting in greater charge carrier recombination and low quantum efficiencies. The application of a positive electrical bias to the photoanode should serve to remove the conduction band electrons and therefore limit undesirable recombination of the charge carriers.

Fig. 4 shows the degradation of formic acid with time for an initial concentration of 3.18×10^{-3} mol dm^{-3}, under conditions of air and O_2 sparging, with the anode operating at OC or at +1.0 V. Table 1 summarises the data giving the rate of degradation of formic acid under the various conditions investigated. The plot of concentration versus time (Fig. 4) gives a straight-line fit and the reaction obeys pseudo zero order kinetics with respect to formic acid. Under air saturated conditions the application of +1.0 V gives enhanced the efficiency of degradation by a factor of 1.3 over OC conditions. In O_2 saturated conditions the application of +1.0 V increased the degradation rate by a factor of only 1.06 compared to rate under OC conditions.

Fig. 5 shows the degradation of formic acid with time for an initial concentration of 6.36×10^{-3} mol dm^{-3} under conditions of OFN, air, and O_2 sparging, with the anode operating at OC or at +1.0 V. The data for the experiments is summarised in Table 1. In air saturated conditions the application of +1.0 V to the anode increased the rate of degradation by a factor of 1.37, while in O_2 saturated conditions the application of +1.0 V increased the rate by a factor of only 1.09. In the OFN sparged solution (anaerobic) the application of +1.0 V to the anode increased the degradation rate compared to OC conditions by a factor of 4.9, however, it must be noted that little degradation of the formic acid occurred under OC in the OFN sparged solution.

The results are summarised in Table 1. The rate of degradation decreases with decreasing O_2 concentration. This decrease on going from O_2 sparging (100%) to air sparging (20%) is more pronounced for the higher initial concentration of formic acid. This is in line with the theory that at higher pollutant concentration O_2 reduction may become rate limiting, at lower concentrations of O_2. The trend in the effect of applied potential is similar for both concentrations studied. In 100% O_2 the applied bias has only a small positive effect. The O_2 in this case is acting as an efficient electron acceptor removing conduction band electrons and reacting with primary radicals formed by the one electron oxidation of formic acid. Recently Hidaka et al. [12] reported that the application of a positive bias of +0.3 V to a Degussa P25-ITO electrode actually resulted in a lower rate of degradation of sodium dodecylbenzenesulphonate and benzenesulphonate as compared to the OC electrode.

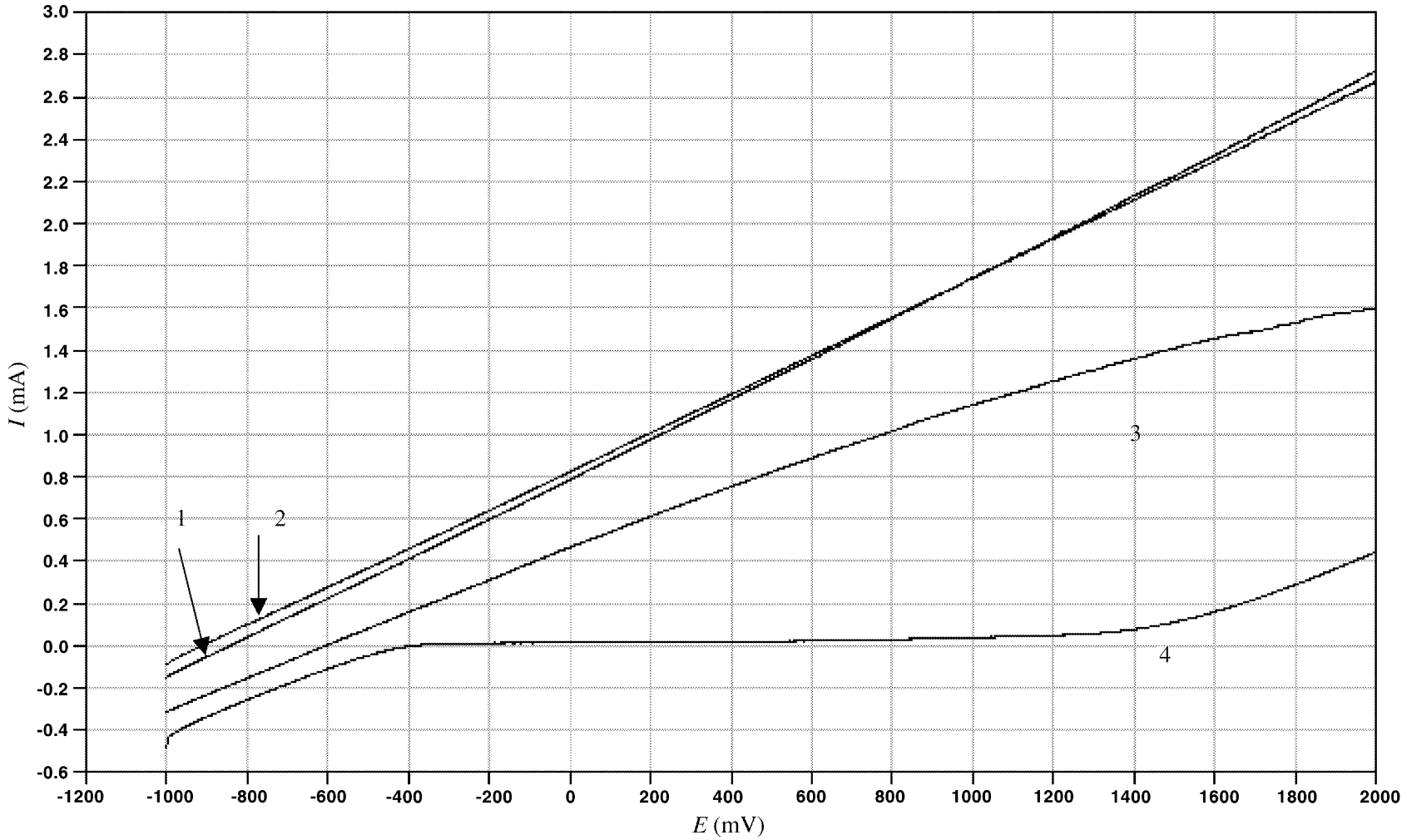

Fig. 3. Linear sweep voltammograms measured in the one-compartment flow cell. Formic acid was present in the cell at 6.36×10^{-3} mol dm^{-3}, sweep rate = 10 mV s^{-1}: (1) air sparged, light; (2) OFN sparged, light; (3) O_2 sparged, light; (4) O_2 sparged, dark.

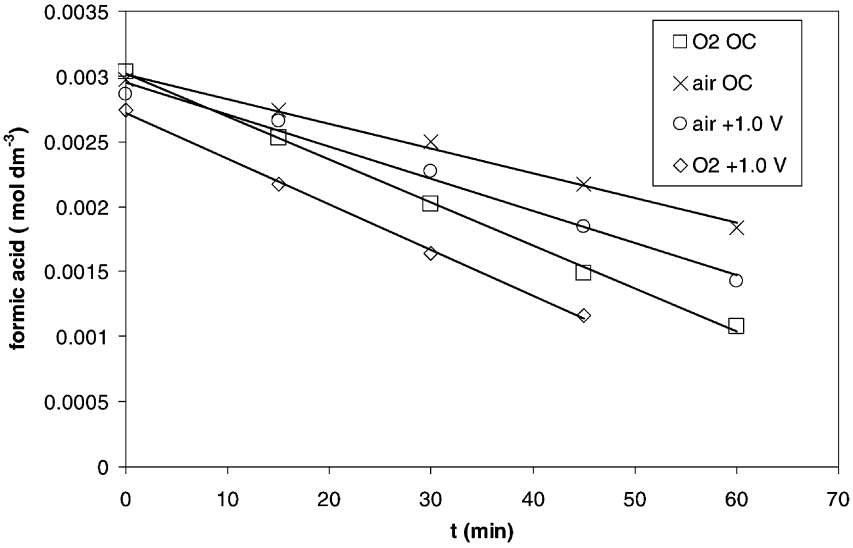

Fig. 4. Formic acid degradation over time for the electrode at OC and +1.0 V in air sparged and O_2 sparged solutions. Initial concentration of formic acid was 3.18×10^{-3} mol dm^{-3}.

In 20% O_2 conditions the reduction of O_2 is rate limiting and the application of a positive bias increases the rate more markedly. However, the rate under applied bias in air sparged solutions remained lower than that measured under O_2 saturated conditions. In anaerobic OFN sparged conditions the application of a positive bias increases the rate by a much bigger margin and the rate was not much less than that observed for the OC electrode in air sparged solution. In the OFN sparged solution the electrons are passed on to residual O_2 or H^+ are reduced at the CE.

Kim and Anderson [11] reported the photocatalytic and photoelectrocatalytic degradation of formic acid using sol-gel derived TiO_2 tin oxide electrodes. They reported an increase in the rate by a factor of 1.3 in oxygenated solutions at a potential of +0.3 V (SCE) as compared to the OC electrode. For OFN sparged solutions they reported an increase in the rate by a factor of 2.8. In another study using a similar system they reported an increase in the degradation rate by a factor of 2 in oxygenated solutions at +0.3 V (SCE) compared to the OC electrode [10].

3.4. OC potential

It has been reported that removal of conduction band electrons may be rate limiting [26]. This effect is illustrated in the OC experiments where the OC potential (E_{OC}) of the electrode was recorded over time (Fig. 6). The E_{OC} in OFN sparged solution was −723 mV and the electrode remained negatively charged for the duration of the experiment. Indeed, even after the lamp was switched off the electrode remained charged. This negative charge is due to photogenerated electrons becoming trapped in the conduction band in the absence of an efficient electron acceptor, therefore raising the fermi potential (E_f) of the TiO_2 electrode. In air sparged solution the E_{OC} was less negative at −610 mV due to O_2 removing photogenerated electrons from the TiO_2 or reacting with primary radicals preventing electron injection into the TiO_2 conduction band. In O_2 saturated conditions the E_{OC} was even less negative at −458 mV and became more positive as time proceeded as the formic acid concentration decreased. This negative charge build up even under

Table 1
A summary of the main data from the photocatalytic and electrochemically assisted photocatalytic degradation in the one-compartment cell

Experiment	Conditions	$[\text{Formic acid}]_{\text{initial}} \times 10^3$ (mol dm^{-3})	O_2 (%)	$E_{\text{anode(initial)}}$ (mV)	E_{cell} (mV)	$I_{\text{ph,ss(initial)}}$ (mA)	Rate (mol dm^{-3} min^{-1})	Φ_{app} (%)
1	Air (OC)	3.18	20	−831	NA	NA	1.9E − 05	2.77
2	Air (+1.0 V)	3.18	20	1000	1.5	2.069	2.46E − 05	3.58
3	O_2 (OC)	3.18	100	−642	NA	NA	3.31E − 05	4.82
4	O_2 (+1.0 V)	3.18	100	1000	1.205	1.682	3.52E − 05	5.12
5	OFN (OC)	6.36	1	−720	NA	NA	2.42E − 06	0.35
6	OFN (+1.0 V)	6.36	1	1000	1.832	1.774	1.18E − 05	1.72
7	Air (OC)	6.36	20	−605	NA	NA	2.16E − 05	3.15
8	Air (+1.0 V)	6.36	20	1000	1.565	1.77	2.97E − 05	4.32
9	O_2 (OC)	6.36	100	−466	NA	NA	4.59E − 05	6.68
10	O_2 (+1.0 V)	6.36	100	1000	1.232	1.1	4.98E − 05	7.26

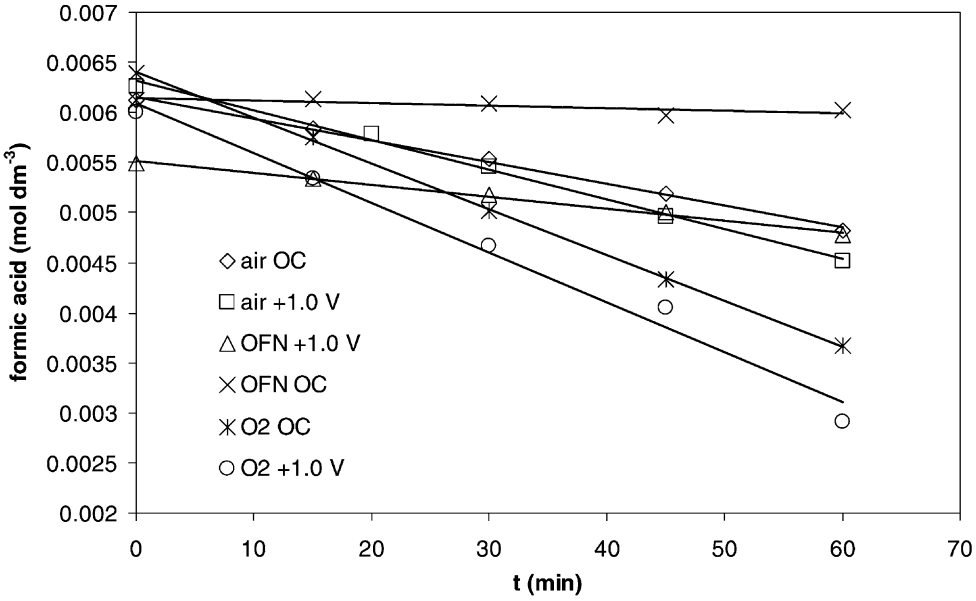

Fig. 5. Formic acid degradation over time for the electrode at OC and +1.0 V in OFN sparged, air sparged, and O_2 sparged solutions. Initial concentration of formic acid was 6.36×10^{-3} mol dm^{-3}.

O_2 saturated conditions indicates that removal of conduction band electrons is indeed slower than hole transfer to solution as proposed by Gerischer and Heller [26].

3.5. Photocurrent

The photocurrent recorded for the experiments employing the higher initial concentration of formic acid under applied bias are shown in Fig. 7. In the OFN and air sparged solutions the photocurrent attained ~1.8 mA and remained fairly static for the duration of the experiment. In the O_2 saturated solution however, the initial photocurrent was 1.1 mA and dropped steadily over the duration of the experiment. Again the lower photocurrent observed for the O_2 saturated experiment was due to the radical and electron scavenging properties of the O_2 at higher concentrations. It is misleading to report Faradaic efficiencies for this system because of photocurrent quenching by O_2 e.g. in O_2 sparging experiment the ratio for measured to calculated Faradaic conversion was 1561%, although in the OFN system it was more reasonable at 151%. It is more appropriate to report the incident photon to current efficiency

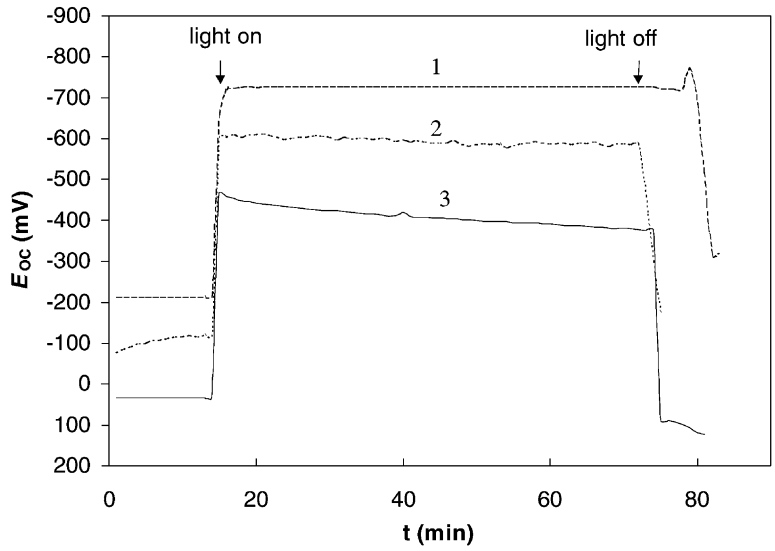

Fig. 6. OC potential of TiO_2 electrode over time. Initial concentration of formic acid was 6.36×10^{-3} mol dm^{-3}: (1) OFN sparged; (2) air sparged; (3) O_2 sparged.

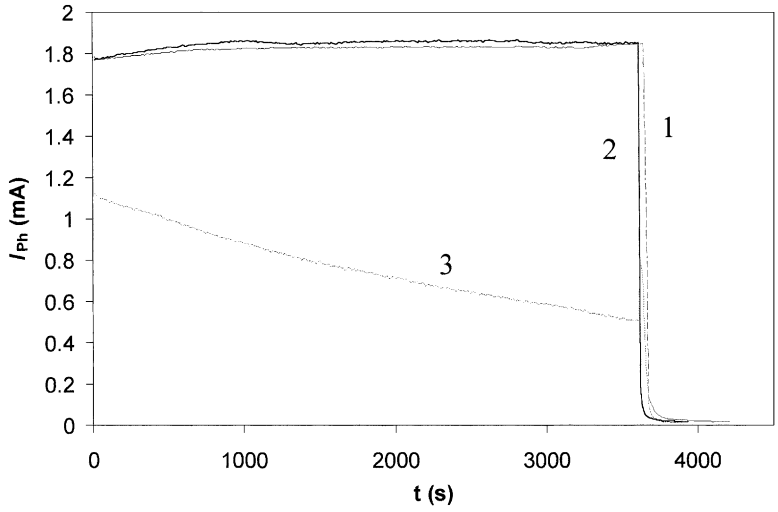

Fig. 7. Photocurrent measured during electrochemically assisted photocatalytic degradation of formic acid. Initial concentration of formic acid was 6.36×10^{-3} mol dm^{-3}. Applied potential was +1.0 V: (1) OFN sparged; (2) air sparged; (3) O_2 sparged.

(IPCE).

$$\text{IPCE} = \frac{j}{[I_0 F]} \tag{2}$$

For this system the IPCE at +1.0 V was low at only 2.2% for the OFN and air sparged solutions and 1.4% for the O_2 sparged solution. The low IPCE under OFN indicates a high recombination rate of charge carriers probably due to a rate limiting cathodic reaction. Previously we reported an IPCE of 10% measured on a TiO_2–Ti-alloy electrode in oxalate solution at a similar light intensity though in a different system [25].

4. Quantum yield

The IPCE mentioned above is a measure of the quantum yield for minority charge carriers, however, in this system the IPCE is low due to electron and radical scavenging by O_2, and, in the absence of an efficient electron acceptor, charge carrier recombination. The apparent quantum yield for the degradation of formic acid was calculated as:

$$\Phi_{\text{app}} = \frac{\text{rate of degradation (mol s}^{-1}\text{ cm}^{-2})}{\text{photon flux (einstein s}^{-1}\text{ cm}^{-2})} \tag{3}$$

The values for Φ_{app} are summarised in Table 1. The IPCE value for O_2 sparged solutions was low, however, Φ_{app} is quite high at around 7% for the higher initial concentration of formic acid.

Candal et al. [16] recently reported a study of the degradation of formic acid in a concentric tube one-compartment PEC utilising a nano-crystalline TiO_2 titanium foil electrode under front face illumination. The CEs were three reticulated vitreous carbon rods. They reported an increase in the rate of degradation of formic acid (in NaCl supporting electrolyte) by a factor of 1.3 at +1.0 V (SCE) compared to the OC electrode. Φ_{app} was found to be 3.6%. Under OFN sparged conditions they were unable to apply a potential of 1.0 V to the anode as the cell potential had increased to >31 V, the limit of their potentiostat. When a potential of 2.0 V was applied to the anode in oxygenated solution the cell potential was measured at 4.4 V. In our system using a platinised titanium CE the cell potential under OFN sparged conditions with the anode at +1.0 V was measured to be only 1.8 V. In oxygen sparged solution with the anode at +1.0 V the cell potential was measured at 1.2 V (Table 1). The lower cell potentials in our system are due to the lower overpotentials required for O_2 and H^+ reduction on platinum and the lower *IR* drop across the cell as the electrodes are of similar dimensions and in a flat plat configuration.

4.1. Simultaneous photocatalytic oxidation of formic acid and recovery of copper in a two-compartment reactor

Previously we reported the simultaneous photocatalytic oxidation of oxalate and the recovery of copper in a two-compartment cell [19]. That study was carried out in a two-compartment cell separated by a porous glass frit and with a TiO_2–titanium-alloy electrode. The current study was designed to take the feasibility of concept one step further by the use of anion exchange membrane to separate the solutions, low power fluorescent lamps as the illumination source, and TiO_2–FTO glass under back-face illumination as the photoanode.

Fig. 8 shows the concentration of formic acid in the anodic half cell as a function of time. The best line fit gave a degradation rate of 2.87×10^{-5} mol dm^{-3} min^{-1} which is similar to the rate determined in the one-compartment cell for the air sparged 6.36×10^{-3} mol dm^{-3} formic acid solution with a bias of +1.0 V. Φ_{app} for formic acid in the

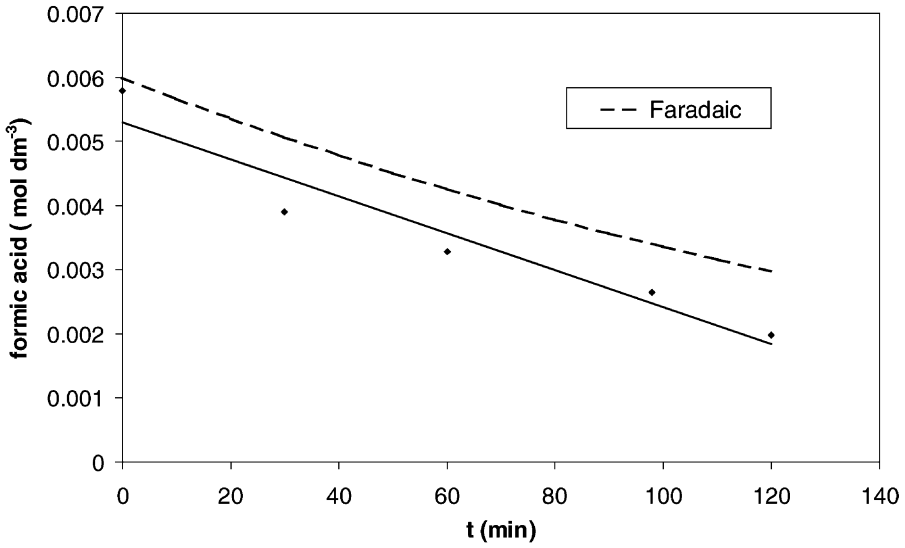

Fig. 8. Formic acid degradation on TiO_2 anode short-circuited to copper CE in the two-compartment PEC with Cu^{2+} as the electron acceptor. The initial concentration of formic acid was 6.0×10^{-3} mol dm^{-3}. Faradaic: the formic acid degradation as calculated using the measured short-circuit photocurrent.

two-compartment system was 3.72%, however, the initial IPCE was 9.5%. The amount of copper recovered was determined by the gravimetric analysis of the copper mesh cathode. Following 120 min the weight of the copper cathode had increased by 13.2 ± 0.2 mg which equates to a decrease in Cu^{2+} concentration by 3.25×10^{-3} mol dm^{-3}. In the same time the formic acid concentration had decreased by 3.82×10^{-3} mol dm^{-3}. The photocurrent was recorded over the duration of the experiment and the Faradaic yield was calculated where the total charge passed is given by:

$$Q = \int I_{sc}\,dt = mnF \quad (4)$$

where I_{sc} is the short-circuit photocurrent (C s^{-1}), n the number of electrons transferred, F the Faraday constant (96 485 C mol^{-1}), and m the number of moles of reactant consumed or product formed.

The short-circuit photocurrent in this reactor was much larger than that observed in the one-compartment reactor with the initial steady state current upon illumination at ~7.6 mA. The total charge passed over the period of the experiment corresponded to the removal of 2.17×10^{-4} mol assuming a $2e^-$ oxidation/reduction. The Faradaic yield for formic acid degradation was 126% which is rather high and may be explained by photocurrent losses due to residual O_2 in the anode. The Faradaic yield for copper recovery was 95.5% which is in good agreement with our previous study which reported a 94% yield for copper recovery in KCl as the supporting electrolyte [19].

The Faradaic removal as calculated is also shown in Fig. 8 for comparison with the formic acid concentration as measured. This reactor set-up needs further experimental investigation but the positive results take the feasibility of concept one step further towards the actual application.

5. Conclusions

Nano-crystalline TiO_2 electrodes prepared by the electrophoretic immobilisation of Degussa P25 on tin oxide glass showed high efficiencies for the degradation of formic acid in one- and two-compartment PECs. The application of +1.0 V to the TiO_2 electrode resulted in a marked increase in the rate of degradation of the formic acid when the concentration of dissolved O_2 was low. There was not a marked increase in the rate in O_2 saturated solutions compared to the OC electrode.

In a two-compartment PEC formic acid was photocatalytically degraded at the anode while Cu^{2+} was reduced to Cu^0 at the cathode when the illuminated TiO_2 anode was short-circuited to the copper mesh cathode. The initial IPCE under for this system was 9.5%. Further experimentation is required to determine if this technology would work with 'real' industrial effluents and solar illumination may be a possibility.

Acknowledgements

The authors wish to thank the European Commission for funding the PCATIE Project (contract no. ENV4-CT97-0632), Degussa for supplying free samples of P25, NIBEC for supplying free samples of ITO glass, and the School of Electrical and Mechanical Engineering at the University of Ulster for constructing the reactors. Also we wish to thank Mr. Robin Ritchie for his technical support in the laboratory.

References

[1] A. Mills, S. Le Hunte, J. Photochem. Photobiol. A 108 (1997) 1–35.
[2] J.A. Byrne, B.R. Eggins, N.M.D. Brown, B. McKinney, M. Rouse, Appl. Catal. B 17 (1998) 25–36.
[3] K. Vinodgopal, S. Hotchandani, P.V. Kamat, J. Phys. Chem. 97 (1993) 9040–9044.
[4] K. Vinodgopal, U. Stafford, K.A. Gray, P.V. Kamat, J. Phys. Chem. 98 (1994) 6797–6803.
[5] K. Vinodgopal, P.V. Kamat, Solar Energy Mater. Solar Cells 38 (1995) 401–410.
[6] R. Pelegrini, P. Peralta-Zamora, A.R. de Andrade, J. Reyes, N. Duran, Appl. Catal. B 22 (1999) 83–90.
[7] J. Rodrigez, M. Gomez, S.E. Lindquist, C.G. Granqvist, Thin Solid Films 360 (2000) 250–255.
[8] S.A. Walker, P.A. Christensen, K.E. Shaw, G.M. Walker, J. Electroanal. Chem. 393 (1995) 137–140.
[9] P. Mandelbaum, S.A. Bilmes, A.E. Regazzoni, M.A. Blesa, Solar Energy 65 (1999) 75–80.
[10] D.H. Kim, M.A. Anderson, J. Photochem. Photobiol. A 94 (1996) 221–229.
[11] D.H. Kim, M.A. Anderson, Environ. Sci. Technol. 28 (1994) 479–483.
[12] H. Hidaka, K. Ajisaka, S. Horikoshi, T. Oyama, K. Takeuchi, J. Zhao, N. Serpone, J. Photochem. Photobiol. A 138 (2001) 185–192.
[13] H. Hidaka, K. Ajisaka, S. Horikoshi, T. Oyama, K. Takeuchi, J. Zhao, N. Serpone, Catal. Lett. 60 (1999) 95–98.
[14] H. Hidaka, K. Ajisaka, S. Horikoshi, T. Oyama, K. Takeuchi, J. Zhao, N. Serpone, J. Photochem. Photobiol. A 109 (1997) 165–170.
[15] I.U. Haque, J.F. Rusling, Chemosphere 26 (1993) 1301–1309.
[16] R.J. Candal, W.A. Zeltner, M.A. Anderson, Environ. Sci. Technol. 34 (2000) 3443–3451.
[17] N.S. Foster, G.N. Brown, R.D. Noble, C.A. Koval, in: D.F. Ollis, H. Al-Ekabi (Eds.), Photocatalytic Purification and Treatment of Water and Air, Elsevier, Amsterdam, 1993, pp. 365–373.
[18] G. Rmachandraiah, S.K. Thampy, P.K. Narayanan, D.K. Chauhan, R.N. Nageswara, V.K. Indusekhar, Sep. Sci. Technol. 31 (1996) 523–532.
[19] J.A. Byrne, B.R. Eggins, W. Byers, N.M.D. Brown, Appl. Catal. B 20 (1999) L85–L89.
[20] J.K.N. Mbindyo, M.F. Ahmadi, J.F. Rusling, J. Electrochem. Soc. 144 (1997) 3153–3158.
[21] T. Freund, W.P. Gomes, Catal. Rev. 3 (1969) 1.
[22] D.J. Fermin, E.A. Ponomarev, L.M. Peter, Proc. Electrochem. Soc. 97 (20) (1997) 61.
[23] J.A. Byrne, B.R. Eggins, S. Linquette-Mailley, P.S.M. Dunlop, Analyst 123 (1998) 2007–2012.
[24] V.S. Bagotzky, Y.B. Vasilyev, Electrochim. Acta. 9 (1964) 869.
[25] J.A. Byrne, B.R. Eggins, J. Electroanal. Chem. 457 (1998) 61–72.
[26] H. Gerischer, A. Heller, J. Phys. Chem. 95 (1991) 5261–5267.